International Journal of Architectural, Civil and Construction Sciences
ISSN: 2415-1734
Vol:9, No:2, 2015

Structural Assessment of Low-rise Reinforced Concrete Frames under Tsunami Loads

Hussain Jiffry, Kypros Pilakoutas, Reyes Garcia

***Abstract*—**This study examines analytically the effect of tsunami loads on reinforced concrete (RC) frame buildings. The impact of tsunami wave loads and waterborne objects are analyzed using a typical substandard full-scale two-story RC frame building tested as part of the EU-funded Ecoleader project. The building was subjected to shake table tests in bare condition, and subsequently strengthened using Carbon Fiber Reinforced Polymers (CFRP) composites and retested. Numerical models of the building in both bare and CFRP-strengthened conditions are calibrated in DRAIN-3DX software to match the test results. To investigate the response of wave loads and impact forces, the numerical models are subjected to nonlinear dynamic analyses using force time-history input records. The analytical results are compared in terms of displacements at the floors and at the "impact point" of a boat. The results show that the roof displacement of the CFRP-strengthened building reduced by 63% when compared to the bare building. The results also indicate that strengthening only the mid-height of the impact column using CFRP is more effective at reducing damage when compared to strengthening other parts of the column. Alternative solutions to mitigate damage due to tsunami loads are suggested.

***Keywords*—**Tsunami loads, hydrodynamic load, impact load, waterborne objects, RC buildings.

I. Introduction

ON 24th December 2004 the Indian Ocean earthquake (M_w=9.3) hit the west coast of Sumatra and caused a tsunami which caused 250,000 fatalities in 12 countries, including Sri Lanka. Sri Lanka did not have any tsunami defense systems or mitigation measures. As a result, the tsunami produced severe devastation along the coast of East (Batticaloa) and South (Galle), which economies rely heavily on tourism. This was Sri Lanka's most devastating natural disaster ever recorded. The total economic loss is estimated in more than US $900 million, i.e. approximately 4.5% of Gross Domestic Product (GDP) [1]. The negative effects of the tsunami also caused a reduction of GDP growth by 1% in 2005. In the aftermath of the tsunami, coastline structures were quickly built to speed up recovery of touristic facilities. However, many of these structures were built using poor construction standards. Moreover, many of these structures have ground floors with elevated columns to allow 'free flow' of tsunami waves. Such exposed columns can be vulnerable to tsunami wave loads (hydrodynamic and impulsive) and impact forces of waterborne objects, and thus may experience damage during future tsunamis. As a result, the resilience of those buildings to resist future potential tsunami loads can be questionable [2]. This is especially true for impact forces due to waterborne objects, which can cause severe damage or even partial structural collapse as shown in Fig. 1.

Fig. 1 Damage on a column due to tsunami waterborne object [3]

Previous studies have examined the effect of tsunami loads on structures, especially on well-designed new buildings [4]. One of the main conclusions from these studies is that well seismically-designed buildings have sufficient strength to withstand tsunami forces without experiencing significant damage. However, limited studies have examined analytically the effect of tsunami loads on substandard structures as those located in Sri Lanka. Hence this paper assesses analytically the effect of tsunami loads on a sub-standard two-story reinforced concrete (RC) frame building as those typically built in Sri Lanka during the post-tsunami reconstruction. The building is modeled and analyzed using DRAIN-3DX software. Numerical analyses are performed to examine the response of the RC frame under tsunami forces (hydrodynamic, impulsive and impact forces of waterborne objects) applied on an exposed open ground floor assuming the structure is situated 500m from the coastline which is higher than the buffer zone allowed in the coast of Weligama, Sri Lanka. The results from the numerical analyses are compared and discussed in terms of displacements at the floors and at the "impact point" of a boat.

II. Estimation of Tsunami Loads

Typical tsunami-induced force components include hydrostatic, hydrodynamic, surge, buoyant, drag force, impulsive and debris impact forces. However, not all these loads act simultaneously on a structure. In this study, only hydrodynamic, impulsive tsunami wave forces and impact force due to waterborne objects are considered as the magnitude of these forces are expected to be large and usually

Mr Hussain Jiffry is with the Department of Civil and Structural Engineering, The University of Sheffield, Sheffield, S1 3JD, UK (phone: 00970526814893; (e-mail: mhmohamedjiffry1@sheffield.ac.uk).

Prof Kypros Pilakoutas and Dr Reyes Garcia are with Department of Civil and Structural Engineering, The University of Sheffield, Sheffield, S1 3JD, UK (e-mail: k.pilakoutas@sheffield.ac.uk, r.garcia@sheffield.ac.uk).

dominate the response. The following sections summarize current standard procedures for the calculation of such forces.

A. Hydrodynamic Force

A moving tsunami wave with a velocity acts on a structural element for a certain period of time during inundation, thus applying a drag force which can be considered as a hydrodynamic force F_H [5]. The force F_H applied at the inundation depth h is given by.

$$F_H = 0.5\rho C_d B(hu^2) \quad (1)$$

where: ρ = fluid density of tsunami flow (=1200 kg/m^3); Cd = drag coefficient (Cd = 2 for square and rectangular columns); B = the breadth of structure in the plane normal to the direction of flow (in meters); hu^2 = momentum flux per unit mass (u = flow velocity; h = flow depth).

The most important parameter on tsunami loading is the velocity of the tsunami flow which influences both hydro-dynamic and impact force loadings. The velocity depends on the inundation depth. The fundamental expression for the velocity is $u= k\sqrt{(gh)}$. Different authors give different values of k [6]-[8]. The velocity obtained by assuming k = 2 relates to the conventional solution of the leading tip of a surge on a frictionless horizontal plane caused by a dam break with the quiescent impoundment depth of h [12]. However, [8] argues that the latter approach may be too conservative, as the computed tip velocity does not represent the velocity of a flow depth h. Therefore, Yeh concludes that the value $k\sqrt{(gh)}$ is not appropriate to represent the flow velocity for a tsunami flood passing through a structure [12]. Instead, [9] proposes the following simplified equation that depends on the parameters taken from the data of the region of study.

$$(hu^2) = gR^2\left(0.125 - 0.235\frac{z}{R} + 0.11\left(\frac{z}{R}\right)^2\right) \quad (2)$$

where: R = maximum run-up height; Z = elevation from shoreline level; g = gravitational acceleration.

Equation (2) was used by [4] to examine the response of buildings due to tsunami loads, and it is also used in this study to calculate the hydrodynamic force. The parameters from the region of study used in the calculations are: maximum run-up height R=11.0 m, inundation depth h=2.5 m and elevation Z=2.0 m.

B. Tsunami Wave Impulsive Force

The main tsunami load during inundation is the impulsive force which acts suddenly at the tip of the wave when the wave hits the structure. This force is also known as 'surge force'. The Japanese guidelines [10] suggest considering this load as 3h of the hydrostatic load. Nonetheless, [8] defines the impulsive load as $1.5\rho gh$ at the inundation height, and $0.5\rho gh$ at the base level of the structure. The latter approach is used in this study to estimate the impulsive force.

C. Debris Impact Force Due to Waterborne Object

A high velocity tsunami travelling in land usually carries heavy debris that can impact structures and cause larger forces than those induced by the tsunami waves. Thus, debris impact loads due to waterborne objects are usually more damaging during tsunamis. Current design guidelines (e.g. FEMA P646 (FEMA 2008) and ASCE 7-10 (ASCE 2010)) provide guidance to determine the peak impact force on a structure.

According to FEMA P646, the peak force can be calculated using the '*contact stiffness*' approach (3), where the contact stiffness is obtained with reference to the properties of the impact object and the structural element.

$$F_P = C_m v\sqrt{k_{eff}}\, m \quad (3)$$

where: C_m = mass coefficient; k_{eff} = effective contact stiffness; v = velocity of the object at the point of impact; m = mass of the object.

Conversely, ASCE 7-10 is based on the principle of *'impulse momentum'* and assumes a half sine pulse as the impact time-history (see (4)). The force is assumed to increase from 0 to F_p at time intervals of Δ=0.003s, decreasing to zero at the 'restitution phase' [11].

$$F_p = \frac{(\pi m v)}{(2\Delta t)} \quad (4)$$

where, Δt = time to decrease object velocity to zero in the compression phase.

To show the inconsistencies between the results yielded by the FEMA P646 and ASCE 7-10 approaches, a 20' shipping container with a tare weight of 2200 kg impacting on a column at a velocity of 6 m/s is assumed. ASCE 7-10 estimates a peak impact of 10,900 kN, whereas FEMA P646 estimates a force of 691 kN using k_{eff}=1.5x10^9 N/mm^2. This inconsistency suggests that the load needs to be thoroughly analyzed using alternative numerical methods [11]. Therefore, this study uses the numerical approach by [11], who provided a set of peak impact forces due boats and shipping containers for analysis purposes. In this study, a boat of 1,500kg was assumed to impact the ground floor of the analyzed structure at an inundation height of 2.5 m (Fig. 2).

Table I summarizes the forces considered in the analysis of the structure, as well as their duration and impact heights. As this study mainly focuses on the effectiveness of strengthening in the case of 'critical' damage, both hydrodynamic and tsunami wave impulsive loads are be analyzed together, whereas debris impact force will be analyzed separately.

III. Characteristics of Case Study Structure

The building considered in this study is the substandard full-scale two-story one-bay RC frame building shown in Fig. 2. The structure was built using inadequate construction practices as those used to build structures in Sri Lanka. The structure was subjected to a series of shaking table tests to assess the effectiveness of CFRP strengthening solutions for

developing countries as part of the EU-funded Ecoleader project [13].

Full details of the Ecoleader building can be found in [13] and only a summary is given in the following.

TABLE I
INPUT PARAMETERS FOR CALCULATED TSUNAMI LOADS

Load type	Duration (s)	Force (kN)	Impact height (m)
Hydrodynamic	14.0	25.0	1.25
Tsunami wave impulsive	0.6	44.0	2.5
Debris impact force	0.1	234.0	2.0

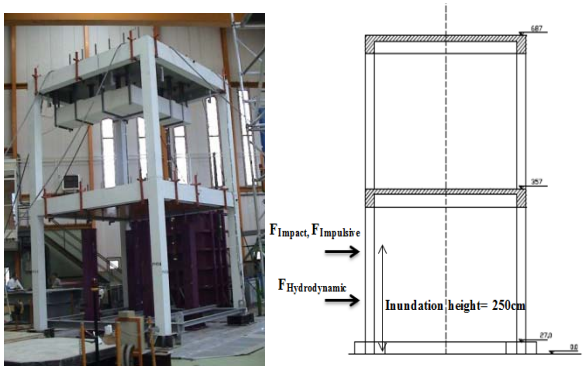

Fig. 2 View of case study structure and corresponding 2D model [13]

The frame had a total height of 6.87m, whereas the cross section of columns and beams was 260x260mm and 260x400 mm, respectively. The slab thickness was 120mm. The concrete strength was 19.6 and 22.1 MPa for all 1st and 2nd floors, respectively. The longitudinal reinforcement used in beams and columns consisted of 14 mm bars with a yielding limit f_y=551 MPa, whereas the transverse stirrups consisted of 8 mm bars and f_y=582 MPa.

The bare frame was initially subjected to a series of shake table tests using records of increasing Peak Ground Accelerations (PGA) ranging from 0.05g to 0.40g. After this, damage in the building was repaired using crack injection and mortar patching. Subsequently, the building was strengthened using CFRP and retested (up to PGA=0.50g) to assess the effectiveness of the strengthening intervention.

IV. MODELING AND CALIBRATION OF ANALYTICAL TOOL

The experimental results recorded during the shaking table tests are used to assess the accuracy of DRAIN-3DX software at predicting the displacement of the tested building. Element 15 was used to simulate the elements of the frame using a distributed plasticity approach. The cross section of beams and columns was discretized in concrete and steel fiber sections to account for the spread of plasticity both along the member and the cross section [4]. The element also allows accumulating strain, thus providing residual deformations. Rayleigh damping is assumed as 3% for both bare and CFRP-strengthened frame modeled in DRAIN-3DX. The stress-strain relationship of unconfined concrete was calculated according to Eurocode-2.

Figs. 3 and 4 compare the 1st and 2nd floor displacements of the bare building calculated during the NTHA with the experimental displacements experienced during the shake table test at PGA=0.30g. It is shown that the analytical predictions compare well with the test results for the different parameters of damping, pullout properties and concrete stress-strain models used in the modeling.

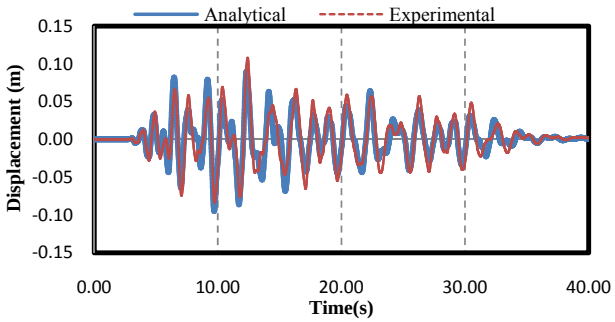

Fig. 3 Displacement-time history of bare frame for 1st floor at PGA=0.30g

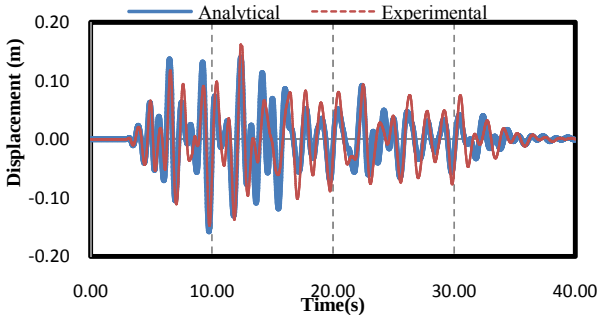

Fig. 4 Displacement-time history of bare frame for 2nd floor at PGA=0.30g

The CFRP-strengthened frame was also calibrated in DRAIN-3DX. The CFRP sheets were modeled by changing the stress-strain constitutive relationship of concrete and by adding the CFRP sheets as additional linear fibers along the elements. The stress-strain relationship of CFRP-confined concrete was calculated according to CEB Model Code 1990.

V. ANALYSIS OF BUILDING UNDER TSUNAMI FORCES

Nonlinear time-history analyses (NTHA) are performed to examine the effect of the tsunami loading on the bare and CFRP-strengthened frame models calibrated in the previous section. Two analyses are considered:

Analysis #1: it takes into account the hydrodynamic tsunami load using a time-history considered by [12]. The time-history load pattern includes 8.0 s of loading, followed by 6.0 s of gradual unloading up to zero load (at 14.0 s), as shown in Fig. 5. Fig. 5 also shows the impulsive load applied during the same analysis at the inundation height (h=2.5m) for a duration of 0.6 s.

Analysis #2: The second analysis considers the load due to waterborne debris impact. The time-history pattern used for this analysis (see Fig. 6) applies a load for 0.1 seconds as recommended by CCH for RC frames. The impact of the boat is assumed to occur on the left column of the 1st floor (ground floor), as shown in Fig. 2. The analysis was performed for 12.0 s.

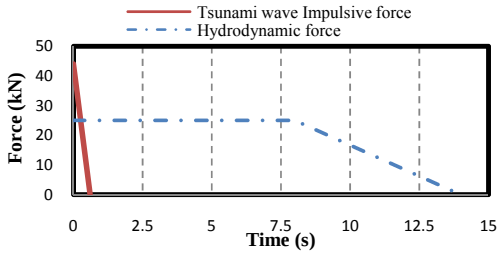

Fig. 5 Force-time history of Analysis #1

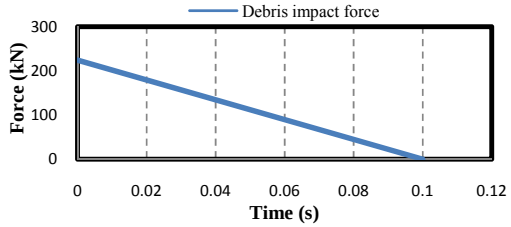

Fig. 6 Force-time history of Analysis #2

VI. Results and Discussion

A. Bare frame

The results from the combined load cases of hydrodynamic and impulsive loading (Analysis #1) for the bare frame are shown in Fig. 7. The plot includes the displacement results at the 1st and 2nd floors, as well as at the impact point where the load is applied (node 1810 in the figure).

The results indicate that the peak roof displacement is 12.8 mm at 0.28 s, whereas the displacement at the impact section is 5.0 mm only and occurs at 0.6 seconds. The application of the loading scenario used in [12] leads to a maximum displacement of 9.4 mm in a two-story RC frame. The results indicate that no yielding of column reinforcement occurs within the duration of the maximum impact. As shown in Fig. 7, the structure experiences negligible negative residual displacement (0.472 mm at 14.0 s).

The bare frame response due to debris impact (Analysis #2) due to a 1,500 kg boat is shown in Fig. 8. Whilst the analysis was performed for 12.0 seconds, Fig. 8 shows results up to 6.0 s only for clarity. The peak displacements at the impact node and at 1st floor are 34.7 and 42.3 mm, respectively. As shown in Fig. 8, such values are recorded at 0.12 s. The results also indicate that the maximum 2nd floor displacement is 58.2 mm and occurs at 0.26 s. This delay of response was expected as the load initially impacts the 1st floor column, whereas the 2nd floor displaces only after the 1st floor reaches its peak displacement. At the end of the analysis, the maximum residual displacement at the 2nd floor was 2.93 mm. Overall; these results indicate that the displacement due to debris impact is considerably larger (by up to 78%) when compared to that produced by the combined effect of hydrodynamic and impulsive loading.

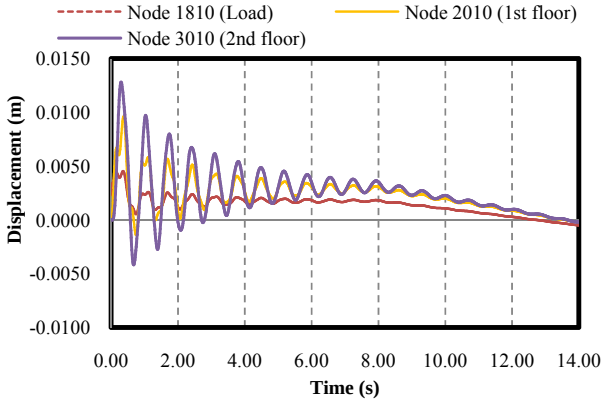

Fig. 7 Displacement-time history of bare frame for Analysis #1

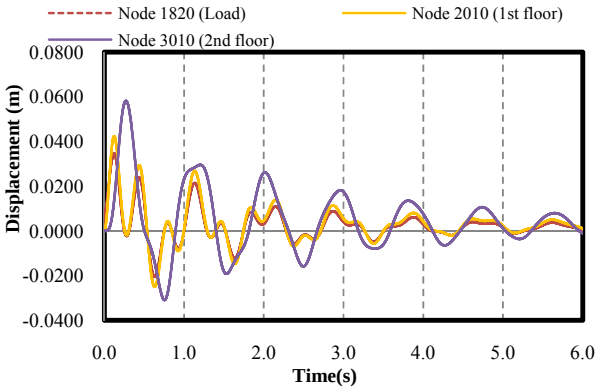

Fig. 8 Displacement time-history of bare frame for Analysis #2

The analytical results also indicated that the maximum strain in the longitudinal bars at the top part of the impact column was 0.0083. This suggests that some plastic activity occurred during the analysis, which may produce excessive rotations at the impact section and lead to potential failure of the column.

The results in Figs. 7 and 8 show that, as expected the maximum amplitude of displacements occurs at the 2nd floor (roof) of the case study building. Hence, the comparison of displacements between bare frame and strengthened frame will only be discussed for 2nd floor and for the Analysis #2 as the impact load can cause more damage (or partial collapse) when compared to Analysis #1. Moreover, damage in buildings and structural performance is commonly associated to the amplitude of displacements (or dirift) at the roof level of the structures.

B. CFRP Strengthened Frame

Analyses #2 was carried out on the CFRP-strengthened model building developed in section IV. However, two cases

were analyzed: (i) the CFRP strengthening applied at the beam-column joints and base of columns as originally done in the Ecoleader building; and (ii) the CFRP strengthening applied at the beam-column joints and at the mid-height of the 1st floor columns (which is vulnerable for impact loads) as shown in Fig. 9.

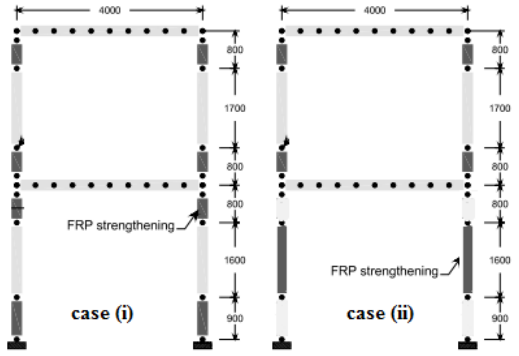

Fig. 9 CFRP strengthening cases analyzed in this study

Fig. 10 compares the maximum 2nd floor displacement of the bare frame and those experienced by the CFRP-strengthened frame for cases (i) and (ii). The results in the figure are cut-off after 6.0 seconds for clarity. Compared to the bare frame response, the strengthening case (i) led to reductions in the maximum displacement of 11.4 mm (20%), whereas the residual displacement dropped by 1.65 mm (56%). Yielding of the longitudinal column reinforcement occurred at the impact section only.

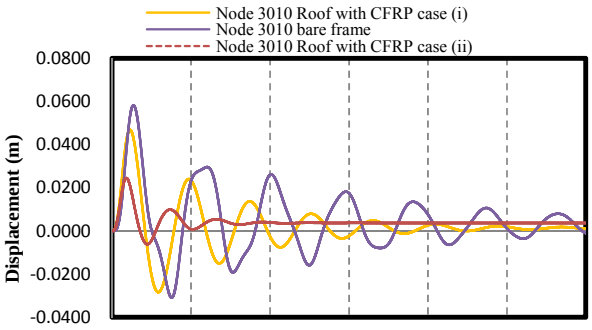

Fig. 10 Comparison of peak displacements of bare frame and strengthened frame for Analysis #2

The results from case (ii) in Fig. 10 indicate a significant reduction of 58% in the maximum displacement compared to the bare frame, and by 47% compared to the frame strengthened only at the joints (case (i)). The reduction in displacements prevented yielding of the longitudinal reinforcement in all elements of the frame. Fig 10 also shows that the residual displacement using strengthening case (ii) is 21% larger when compared to the bare structure. The results also suggest that the structure case (ii) comes to zero displacement (or rest state) faster. This can be attributed to the strengthening and confinement of the impact section, which is the weakest zone of the structure.

In general, the analytical results prove that the CFRP strengthening intervention is very effective at improving the structural behavior of the case study building, thus being an alternative solution to reduce the potential damage of buildings subjected to tsunami loads.

VII. Alternatives to Mitigate Damage due to Tsunami

Whilst this paper has shown the effectiveness of structural strengthening at improving the behavior of a single existing structure subjected to tsunami load, other mitigation solutions are suitable to protect a group of structures in larger tsunami-prone regions. For instance, coastal vegetation or tsunami forests around vulnerable structures can be used to reduce, absorb and dissipate energy from impact forces. This is an environmentally friendly and cost-effective mitigation measure appropriate for developing countries, where the cost of materials such as CFRP may limit their use.

Other more cost-effective strengthening options such post tensioned metal strapping (PTMS) can be used for strengthening [14], but it is still necessary to assess the effectiveness of the PTMS technique at reducing the effect of tsunami forces on buildings.

VIII. Summary and Conclusions

This paper assessed analytically the behavior of existing RC structures subjected to tsunami loads built during the post-tsunami reconstruction in Sri Lanka. From the analysis performed in this study, the following conclusions can be drawn:

1. The dominant effect in a tsunami situation is the impact due to waterborne objects. These results in the bare frame indicate that the displacement due to debris impact is up to 78% larger than that produced by the combined effect of hydrodynamic and impulsive loading.
2. The bare frame building experiences significant displacements (up to 58.2 mm at the 2nd floor) when impacted by a water-borne object. The impact leads to yielding of reinforcement on a ground floor column, which may cause excessive rotations and eventually produce a catastrophic failure.
3. The CFRP strengthening intervention was very effective at reducing potential failure of the strengthened building. The initial analysis (i) with CFRP strengthening at supports reduces moderately the displacement of the building by up to 20%. The application of CFRP at the impact section is more effective at reducing displacements up to 58%. These lower displacements are expected to lead to less damage in the structure.
4. In addition to structural strengthening of single buildings, other alternatives to mitigate potential damage due to tsunamis such as coastal vegetation or tsunami forests can be implemented. These cost-effective and environmentally friendly solutions can absorb and

dissipate energy from impact forces and can be suitable to protect groups of buildings in tsunami-prone regions of Sri Lanka and other developing countries.

REFERENCES

[1] Post Tsunami Recovery and Reconstruction, Joint report of government of Sri Lanka and Development partners (December 2005).

[2] Renuka, I. H. S., and C. S. Lewangamage. (2011) *Structural Aspects Of Post Tsunami Domestic Constructions In Sri Lanka*. Journal of SLSAJ, Vol 11, 65-71

[3] Nistor, I., Palermo, D., Nouri, Y., Murty, T., and Saatcioglu, M., *"Tsunami-Induced Forces on Structures,"* Handbook of Coastal and Ocean Engineering, World Scientific, 2009.

[4] Madurapperuma, K. M. (2007). *Impact Response of Buildings due to Tsunami Water-Borne Massive Objects*. M.Eng. Thesis, Dept. of Civil Engineering, Tokyo Institute of Technology, Tokyo, Japan.

[5] FEMA P646. (2008). *Guidelines for Design of Structures for Vertical Evacuation from Tsunamis.* Washington, D.C., Federal Emergency Management Agency.

[6] Federal Emergency Management Agency (FEMA). (2000). *FEMA coastal construction manual, F*EMA 55,Washington, D.C.

[7] Thurairajah A. (2005). *Structural design loads for tsunami and floods.* International Conference on Disaster Reduction on Coasts, November, Melbourne, Australia.

[8] Yeh H., Robertson I. & Preuss J. (2005). *Development of Design Guidelines for Structures that Serve as Tsunami Vertical Evacuation Sites*. Washington Division of Geology and Earth Resources, Open file report - 4, November, 2005

[9] Yeh, H. (2007). *Design tsunami forces for onshore structures*, J of Disaster Research, 2(6), 531-536.

[10] CCH. (2000). *Regulations within flood hazard districts and developments adjacent to drainage facilities in the revised ordinances of Honolulu,* City and Country of Honolulu Building Code, Department of Planning and Permitting, Honolulu, Hawaii.

[11] Madurapperuma K.M. & Wijeyewickrema A.C. (2008). *Nonlinear response of RC buildings due to impact of tsunami water-borne boats and containers.* 14th World Conference on Earthquake Engineering, International Association for Earthquake Engineering, October, Beijing, China.

[12] Dias, W.P.S., Bandara, K.M.K. (2012),*Tsunami Wave Loading on Buildings: A Simplified Approach,* Department of Civil Engineering, University of Moratuwa, Moratuwa, Sri Lanka,

[13] Garcia R, Hajirasouliha I, Pilakoutas K (2010) *Seismic behaviour of deficient RC frames strengthened with CFRP composites*. Eng Struct 32(10), 3075-3085.

[14] Garcia, R., Hajirasouliha, I., Guadagnini, M., Helal, Y., Jemaa, Y., Pilakoutas, K. et al. (2014) *Full-scale shaking table tests on a substandard RC building repaired and strengthened with Post-Tensioned Metal Straps*. J Earthquake Eng, 18(2), 187-213.